Semiconducting diamonds

V. S. Vavilov and E. A. Konorova

P. N. Lebedev Physics Institute, USSR Academy of Sciences, Moscow
Usp. Fiz. Nauk **118**, 611–639 (April 1976)

A review is given of the current data on semiconducting diamonds, both natural and those prepared by doping in the course of crystal growth in the laboratory or by implantation of impurities in insulating crystals. The review deals with theoretical papers reporting calculations of the principal characteristics of the energy band structure of diamond, and with the results of experimental studies of the energy spectra, photoionization, charged-particle ionization, transport phenomena, and luminescence of semiconducting diamonds. Special attention is paid to the problem of the nature of electrically active acceptor and donor local centers. Actual and potential technical applications of secmiconducting diamonds are discussed briefly.

PACS numbers: 71.30.Mw, 71.50.+t, 72.80.Le, 78.60.Dg

CONTENTS

1. Introduction 301
2. Energy Band Structure of Diamond 301
3. Natural p-Type Semiconducting Diamonds 308
4. Synthetic Semiconducting Diamonds 310
5. Nitrogen Centers in Diamond 312
6. Semiconducting Diamonds Prepared by Ion Implantation Method . . 312
7. Potential Practical Applications of Semiconducting Diamonds . . . 314
Literature 315

1. INTRODUCTION

Well before the birth of modern solid-state physics, diamonds were attracting attention because of their mechanical, optical, and other properties.

Diamond is one of the few "model" very simple nonmetallic crystals. Fundamental investigations of diamond were carried out in the nineteen-thirties. It is sufficient to mention here the experiments of Godden and Pohl on diamonds, which established the basic laws of the internal photoelectric effect, or those of van Heerden *et al.*, who studied the ionization caused by high-energy charged particles. In 1952, Custers[3] found a semiconducting crystal among natural insulating diamonds. Natural semiconducting diamonds always have p-type conduction and are found only very rarely. Nevertheless, the existence of semiconducting diamonds has opened up new opportunities for investigation. The number of papers published on the optical, electrical, and thermal properties of semiconducting diamonds is now large. The work done up to 1964 by a group of British physicists can be found in a book edited by R. Berman, "Physical Properties of Diamond."[1]

There has been considerable progress in preparing synthetic semiconducting diamonds and in doping natural diamonds by ion implantation. In this situation, studies of semiconducting properties of diamond are not only of scientific but also of practical importance because new semiconductor devices can be made of diamond (for example, those operating at high temperatures). Diamond detectors of nuclear particles and thermistors are already in use in some branches of science and technology.

The present authors are not aware of any review on the subject of semiconducting diamonds in the last five years. The aim of the present review is to acquaint physicists (and other specialists investigating applications of solid-state physics) with this semiconducting material which has a unique combination of properties and which will find its place in semiconductor electronics.

2. ENERGY BAND STRUCTURE OF DIAMOND

A. Theoretical investigations

Like germanium and silicon, diamond is a covalent crystal. All these three elements have what is known as the diamond structure.

Each carbon atom in diamond is at the center of a tetrahedron formed by four neighboring atoms. Valence electrons are paired each with one of the valence electrons of the nearest neighbors. The electron cloud of these paired electrons is elongated along the axes joining the atoms. These electron pairs form covalent bonds.

Diamond is one of the first crystals for which calculations were made of the energy band structure, i. e., of the dependence of the energy of electrons on their quasimomentum (or wave vector). All the values of the wave vectors in a crystal lie within a certain volume in the wave vector space, which is known as the Brillouin zone.[4] The Brillouin zone of diamond is shown in Fig. 1. Some of the symmetry points are lettered in Fig. 1. The axes of the Brillouin zone in the wave-vector space correspond to the crystallographic axes. For example, the Γ–X direction corresponds to the [100] axis in the crystal and the Γ–L direction to [111].

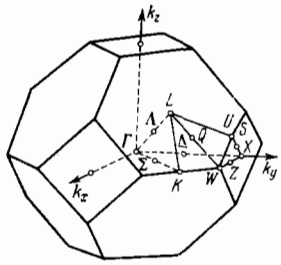

FIG. 1. Brillouin zone of a crystal with diamond structure.

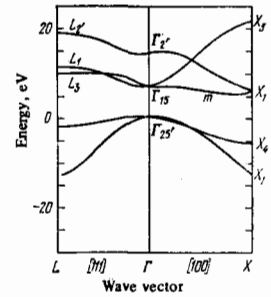

FIG. 2. Energy band structure of diamond.[2]

The first calculations of the energy band structure of diamond were carried out by Herman *et al.*[2] by the orthogonalized plane wave method. The results of calculations for some directions in the Brillouin zone are shown in Fig. 2. The points denoted by Γ correspond to the center of the Brillouin zone, i. e., to zero wave vector, whereas the points X correspond to the boundary of the Brillouin zone along the [100] direction and the points L to the boundary along the [111] axis. It is clear from Fig. 2 that the valence electrons of the carbon atoms form valence bands within which the energy is a continuous function of the wave vector. The valence band of diamond is represented in Fig. 2 by two branches or subbands, which are in contact at the point $\Gamma_{25'}$. At this point, the energy of an electron in the valence band has its maximum value (band edge). The electron states in the upper branch of the valence band are quadruply degenerate and those in the lower branch are doubly degenerate. However, the results of calculations presented in Fig. 2 are obtained ignoring the interaction between the spin and magnetic moment of the orbital motion of electrons. In fact, the upper branch is split into two doubly spin-degenerate subbands, known as the bands of the "light" and "heavy" holes. The degeneracy is lifted except at the center of the Brillouin zone, i. e., at the point $\Gamma_{25'}$. The spin–orbit interaction shifts the lower branch downward in the direction of lower energies. Thus, at the point $\Gamma_{25'}$, the lower subband is split off (spin–orbit band splitting). We shall see later that the experimental value of the splitting of the valence band of diamond is only 0. 006 eV (this should be compared with 0. 28 eV for germanium and 0. 035 eV for silicon).

The excited states of electrons also form bands known as the conduction bands. It is clear from Fig. 2 that there is a considerable energy gap (forbidden band) between the valence and conduction bands. The width of the forbidden band of diamond is considerably greater than the corresponding widths of germanium and silicon and therefore, pure diamond should be a good insulator. The minimum electron energy in the conduction band (band minimum) corresponds to the point m in Fig. 2. However, in the vicinity of this point, the energy varies slowly with the wave vector and, therefore, the calculated position of the conduction-band minimum is not known exactly.

The energy band structure of diamond was also calculated by the pseudopotential method.[3]

The results of the calculations reported in[2] and[3] diverge only slightly and mainly at high values of the wave vector. Experimental investigations of the energy-band structure of diamond have yielded the energy gaps between the valence and conduction bands both at the band edges, i. e., between the valence-band maximum and the conduction-band minimum, and well inside the Brillouin zone (corresponding to nonzero wave vector), and they have made it possible to determine the characteristics of electrons and holes in the bands. As in the case of other semiconductors, the cyclotron resonance method has been found effective. It should be mentioned that the valence band of diamond is fairly thoroughly investigated. However, the information on the conduction band is very limited.

B. Experimental results of optical investigations

1) *Fundamental absorption band edge.* Optical excitation may give rise to electron transitions from the valence to the conduction band and these transitions may be direct or indirect. In the case of direct transitions, the initial and final states have the same value of the quasimomentum K, i. e., in the coordinates (E, K), these transitions are represented by vertical lines; in the case of indirect transitions, the values of K for the initial and final states may be different. In this case, the law of conservation of momentum is satisfied because of simultaneous interaction of electromagnetic radiation with electrons and crystal lattice vibrations (phonons). The transition of an electron from the valence band edge to the conduction-band minimum in diamond is indirect because the values of the quasimomentum of the initial and final states are different (Fig. 2). The experimental results of Clark *et al.*[6] for the temperature dependence of the fundamental absorption band edge of the purest natural diamonds[1)] recorded in the photon energy range 5–6 eV led them to the conclusion that indirect interband transitions and transitions to exciton states took place in this range. Figure 3 shows the spectral dependence of the absorption coefficient at 295 °K; Fig. 4 gives the results obtained by the same authors at different temperatures. At 126 °K, which was the lowest temperature at which measurements were carried out, a steep rise of the absorption began at $h\nu = 5.48$ eV. A similar analysis of the profile of the absorption band edge, based on the theoretical ideas on electron transitions,[5,7] enabled Clark *et al.* to attribute the various parts of the spectral dependence of the absorption coefficient to transitions terminating in ex-

[1)]For historical reasons, insulating diamonds with the lowest nitrogen impurity concentrations are called type IIa and semiconducting diamonds are called type IIb (see Sec. 2a).

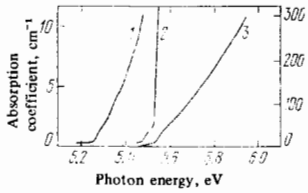

FIG. 3. Absorption spectrum of diamond recorded at 295 °K near the fundamental edge.[6] The ordinate scale on the right applies to curves 2 and 3 but, in the latter case, it should be increased eightfold compared with curve 2.

citon states and to identify three regions corresponding to the annihilation of specific phonons and three regions corresponding to phonon creation.

Unfortunately, at the time of publication of the work of Clark *et al.*,[6] no accurate data were available on the phonon spectrum of diamond. Therefore, the phonon identifications could not be made really reliably. The dispersion curves of phonons in diamond were obtained later[8,9] by the method of inelastic scattering of neutrons. These results were allowed for in studies of recombination radiation[14–16] and this made it possible to refine the energies of phonons participating in electron transitions. The forbidden band width of diamond at 295 °K, corresponding to indirect transitions, can now be regarded as reliably established: $E_g = 5.490 \pm 0.005$ eV. The temperature dependence of E_g, approximated by a linear law near room temperature, can be described by

$$\frac{\Delta E_g}{\Delta T} = -(5.4 \pm 0.5) \cdot 10^{-5} \text{ eV/°K}.$$

2) *Optical studies of electron transitions within allowed bands.* The optical properties of diamond in the photon energy range 5.5–31 eV were investigated in[10–13]. Measurements were made of the reflection from the surface of diamond and the data were then used to calculate the optical constants from the Kramers–Kronig relations. Considerable quantitative discrepancies were found between the results reported in[10] and[11]. As shown in[13], this discrepancy was due to the contamination of the crystal surface. The results of measurements reported in[10] and[13] are identical and should, therefore, be regarded as most reliable. Figures 5 and 6 show the spectral dependences of the reflectivity and absorption coefficient taken from[10]. The reflection maximum at 7.1 eV and the steep rise of the absorption coefficient in the same range of photon energies are attributed in[10,13] to $\Gamma_{25'} \rightarrow \Gamma_{15}$ transitions (Fig. 2) at K = 0. The sharp maximum

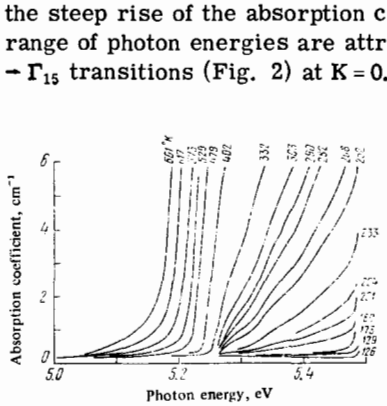

FIG. 4. Absorption edge of diamond at various temperatures.

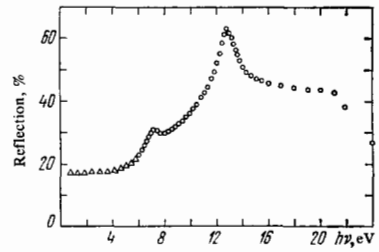

FIG. 5. Reflection spectrum of diamond in vacuum ultraviolet.[10] The values below 5.5 eV were calculated from the refractive index.

in the absorption and reflection curves at 12.5 eV corresponds to the $X_1 \rightarrow X_4$ transition. Similar absorption maxima are exhibited by silicon and germanium and are interpreted in the same way on the assumption that their positions agree well with the calculated data on the forbidden band width at the point X (at this point, the calculations are most reliable).

Figure 7 shows the dependences of the real ε_1 and imaginary ε_2 parts of the permittivity, and of the imaginary part of $1/\varepsilon$ on the photon energy. The function $\mathrm{Im}(1/\varepsilon)$ (known as the loss function) has a maximum at about 30 eV, in agreement with the position of the plasma resonance of the valence electrons in diamond. An analysis of the spectral dependence of ε_2 and the presence of small maxima of the ε_2 reflection curves are used in[13] to identify regions near 16 and 23 eV, which are attributed to the $X_1 \rightarrow X_1$ and $\Gamma_{25'} \rightarrow \Gamma_1$ transitions, respectively. A comparison of the experimental results with the calculated data[2,3] is made in Table 1.[13] The agreement between experiment and theory is good.

3) *Experimental studies of recombination radiation.* The first detailed investigation of the interband recombination radiation of diamond was carried out by Dean and Jones in 1964.[14] Later investigations were reported in[15,16]. In all these cases, the recombination radiation (luminescence) was excited by a beam of accelerated electrons.

Figure 8 shows a typical edge luminescence spectrum of semiconducting diamond recorded at 100 °K.[15] The interpretation of the spectrum in Fig. 8 was made in[15] on the basis of a comparison of the spectra obtained for different samples, experimental data on the edge absorption spectrum,[16] and dispersion curve of the lattice vibrations obtained by the inelastic scattering of neutrons.[8,9] The results are as follows. The stron-

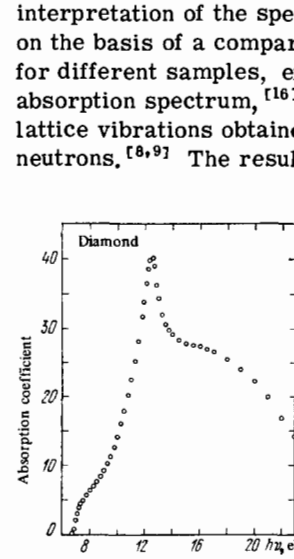

FIG. 6. Spectral dependence of the absorption coefficient (in units of 10^5 cm^{-1}) of diamond in vacuum ultraviolet.[10]

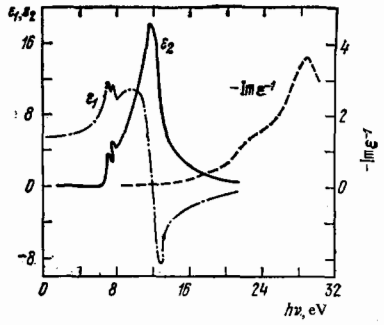

FIG. 7. Spectral dependences of the real and imaginary parts of the permittivity of diamond in vacuum ultraviolet.[13]

gest luminescence maximum (B_1 band) is located at a photon energy of 5.268 eV. The luminescence is due to the annihilation of a free exciton and simultaneous emission of a transverse acoustic phonon of energy $\hbar\omega_{TA} = 0.087$ eV. An analysis of the profiles of the A_1 and B_1 luminescence bands is made on the assumption that the excitons have the Maxwellian energy distribution:

$$J = J_0 \alpha \exp\left[-\frac{(h\nu - h\nu_0)}{kT}\right], \qquad (1)$$

where $h\nu_0$ is the photon energy corresponding to the long-wavelength luminescence threshold, α is the absorption coefficient, and J_0 is the normalization factor.

The results of an analysis of the profiles of the luminescence bands[15] indicate that the A_1 and B_1 bands consist of two unresolved maxima, which are located at photon energies differing by 7 meV (the luminescence bands found in this way are identified in Fig. 8 as B_1 and B_1' and A_1 and A_1'). According to the cyclotron resonance data, the spin–orbit splitting of the valence band is 6 meV,[28] which is in good agreement with the splitting of the luminescence bands A and B. Therefore, it is suggested in[15] that, in this case, the luminescence involves degenerate and split-off valence bands.

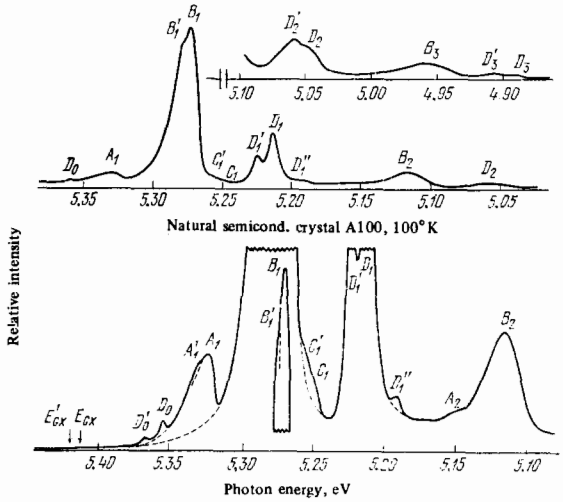

FIG. 8. Recombination radiation (luminescence) spectrum of a natural semiconducting diamond crystal obtained at 100 °K. The spectrum is shown on three different scales.[15]

On the long-wavelength side of the band B in Fig. 1, there are two shoulders, denoted by C_1 and C_1', which are again separated by an energy interval of 7 meV. These shoulders are attributed to the annihilation of a free exciton accompanied by the emission of a longitudinal optical phonon of energy $\hbar\omega_{LO} = 0.163$ eV.

Figure 8 also shows wide maxima B_2 and B_3, separated from B_1 by 0.167 and 2×0.167 eV, respectively. Since 0.167 eV is practically identical with the energy of an optical phonon at $K = 0$, it is natural to attribute the B_2 and B_3 bands to the phonon replicas of B_1. As pointed out in[15], the ratio of the intensities of the zero-phonon transition to the phonon-assisted transition is

$$\frac{J_n}{J_0} = \frac{\Delta E}{\Delta E + n\hbar\omega}\,\gamma_1^n, \qquad (2)$$

where ΔE is the energy of an electron transition, $\hbar\omega$ is the phonon energy, n is the number of phonons participating in the transition, and γ_1 is the phonon–hole

TABLE 1.

Energy (eV) at maximum		Transition	Comments	Theoretical transition energy	
ε_2	$Im(1/\varepsilon)$			acc.[2]	acc.[3]
7.3	–	$\Gamma_{25'} \to \Gamma_{15}$	Transitions along Γ–Δ with threshold at M_0 minimum	6.8	7.8
7.8	–	Indeterminate	Maximum of ε_2 probably due to complex energy structure at Γ	–	–
12.2	–	$X_4 \to X_1$	Wide range of parallel bands near X	11.6	12.9
16			Transitions in wing of 12.2 eV maximum on high-energy side and between parallel bands near X	18.4	24
23	23	$\Gamma_{25'} \to \Gamma_1$ or of impurity origin	Transition sensitive to surface treatment	21.5	–
–	30	Plasma resonance	Experimental value of characteristic losses of 31 eV electrons	–	–

TABLE 2. Principal parameters of interband recombination radiation spectrum of diamond

Designation	Energy, eV	Physical meaning
Lumin. band B_1	5.268	$E_{ex}-\hbar\omega_{TO}^{C}$
" " B_1'	5.275	$E_{ex}'-\hbar\omega_{TO}^{C}$
" " A_1	5.322	$E_{ex}-\hbar\omega_{TA}^{C}$
" " A_1'	5.329	$E_{ex}'-\hbar\omega_{TA}^{C}$
" " C_1	5.346	$E_{ex}-\hbar\omega_{LO}^{C}$
" " C_1'	5.253	$E_{ex}'-\hbar\omega_{LO}^{C}$
" " B_2	5.10	$E_{ex}-\hbar\omega_{TO}^{C}-\hbar\omega_R$
" " B_3	4.93	$E_{ex}-\hbar\omega_{TO}^{C}-2\hbar\omega_R$
$\hbar\omega_{TA}^{C}$	0.087 ± 0.002	Transverse acoustic phonon at $k=k_c$
$\hbar\omega_{TO}^{C}$	0.141 ± 0.001	Transverse optical phonon at $k=k_c$
$\hbar\omega_{LO}^{C}$	0.183 ± 0.001	Longitudinal optical phonon at $k=k_c$
$\hbar\omega_{TA}^{Z}$	0.10 ± 0.005	Transverse acoustic phonon at $k=k_{max}$ [100]
$\hbar\omega_R$	0.167 ± 0.002	Raman phonon ($k=0$)
E_{ex}'	5.416 ± 0.002	Energy of indirect exciton transitions associated with upper valence subbands at 100 °K (average value)
E_{ex}	5.409 ± 0.002	Energy of indirect exciton transitions associated with upper valence subbands at 100 °K
E_{xi}	0.08 ± 0.005	Binding energy of indirect excitons
E_{gi}	5.49 ± 0.005	Forbidden band width for indirect transitions associated with upper valence subbands

interaction parameter.

However, the intensities of the B_1, B_2, and B_3 bands do not satisfy the above relationship. This requires further analysis but it does not mean that we have to reject the hypothesis that the B_2 and B_3 bands are the phonon replicas of the B_1 band. The maxima in the series denoted by D, also clearly visible in Fig. 8, are due to the presence of an acceptor impurity. The main characteristics deduced from the luminescence spectrum are listed in Table 2. The results of experimental studies of recombination radiation and neutron scattering by phonons have refined somewhat the absorption data. Thus, the transition involving a phonon of 0.132 eV energy is excluded from Table 2, because its presence has not been confirmed by subsequent experimental investigations. Figure 9 shows the dispersion curves of the lattice phonons.[18] The crosses denote the energies of the phonons participating in electron transitions. We can see that all these phonons have the same value of the momentum, which governs the position of the conduction-band minimum relative to the valence-band maximum at $k=0.76k_{max}$. This interpretation of the recombination radiation spectrum is in agreement with all the currently available experimental data on electron transitions in diamonds. There is only some doubt about the representation of the A and B maxima as two overlapping bands because an increase in the width may be due to overheating of the samples.[16]

Figure 10 shows the recombination radiation spectrum of a semiconducting diamond at 550 °K.[15] The radiation intensity is much lower than that observed at 100 °K and only the B_1^E and B_2^E bands are well resolved

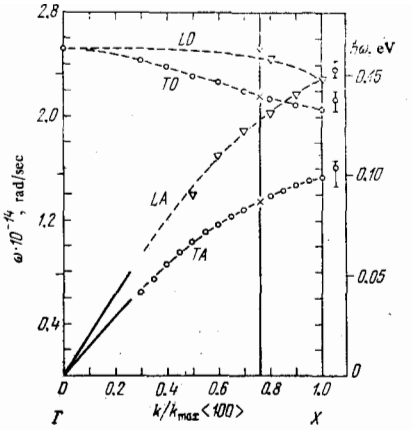

FIG. 9. Dispersion curves of lattice vibrations in diamond along the [100] direction.[18] The vertical line at $k/k_{max}=0.76$ represents the position of the conduction band.

(they correspond to the B_1 and B_2 bands in Fig. 8). An analysis of the B_1^E band reveals additional absorption on the short-wavelength side, which is attributed to the recombination of free electrons and holes. The weak maxima B_1^A and A_1^A are attributed to the annihilation of a free exciton accompanied by the absorption of the relevant phonons (one transverse optical and one transverse acoustic). However, the interpretation of the spectrum in Fig. 10 is much less reliable and should be regarded as only tentative.

C. Effective masses of holes and spin-orbit splitting of valence band of diamond

Cyclotron resonance observations can be used to determine the effective mass of carriers in an energy band.

Since the structure of the valence bands of germanium, silicon, and diamond is similar, we may assume that

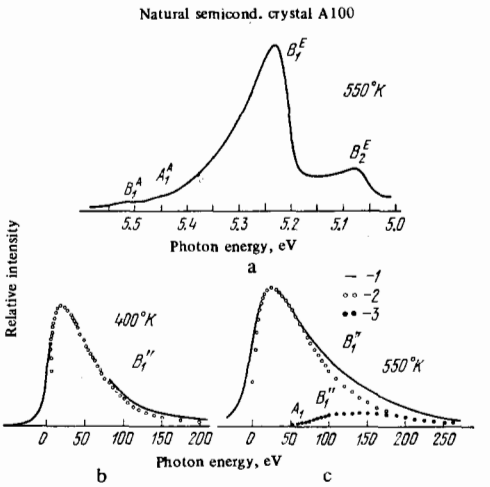

FIG. 10. Recombination radiation (luminescence) spectra of diamond obtained at elevated temperatures[15]: a) general form of the spectrum at 550 °K; b) B band at 400 °K [the circles represent the curve calculated from Eq. (2)]; c) B band at 550 °K [circles denoted by 2 represent the curve calculated from Eq. (2) and circles denoted by 3 are the results of subtraction of the calculated from the experimental curve].

the three valence subbands correspond to three values of the resonance frequencies. According to the theory of Dresselhaus, Kip, and Kittel,[17] the constant-energy surfaces can be described by

$$E = -\frac{h^2}{2m_0}\{Ak^2 \pm [B^2k^4 + C^2(k_x^2k_y^2 + k_y^2k_z^2 + k_z^2k_y^2)]\}; \quad (1)$$

here, k_x, k_y, and k_z are the components of the wave vector; A, B, and C are coefficients; m_0 is the mass of a free electron; h is the Planck constant.

According to this formula, the effective mass can be anisotropic. An investigation of natural semiconducting p-type diamonds in magnetic fields[18] revealed two resonance lines corresponding to the following effective masses of holes:

$$\frac{m^*}{m^0} = (0.70 \pm 0.01) \qquad (H = 17.48 \text{ kOe}),$$

$$\frac{m^*}{m_0} = (1.06 \pm 0.04) \qquad (H = 27.85 \text{ kOe}),$$

These values were obtained for a crystal at 1.2 °K. The carriers were excited optically. Within the limits of the experimental error, the resonant absorption of microwaves was independent of the relative orientations of the electromagnetic field and the crystal axes, which corresponded to the coefficient C in Eq. (1) given by $C^2 < 0.16$. Consequently, the valence subbands of diamonds are almost isotropic, in contrast to those of germanium and silicon which are quite strongly anisotropic.

Additional information was obtained in[19]. In this case, carriers were excited by monochromatic light and this made it possible to follow the dependences of the microwave absorption band intensities corresponding to cyclotron resonance on the photon energy. As in[18], the measurements were carried out on natural semiconducting p-type diamonds. Figure 11 shows the spectral dependences of the intensities of the cyclotron resonance bands in the photon energy range 0.3–0.4 eV. An intersection of a curve with the horizontal axis gave the binding energy of acceptors (the position of the energy level of acceptors measured relative to the edge of the appropriate band). The difference between the photon energies amounted to 0.006 ± 0.001 eV. This difference represented the spin–orbit splitting of the valence band of diamond. Hence, the effective masses obtained should be attributed to the light-hole and split-off bands, respectively.

Heavy holes have a much greater mass. They correspond to a wide cyclotron resonance maximum (Fig. 12). The mass of these heavy holes is

$$\frac{m^*}{m_0} = 2.12.$$

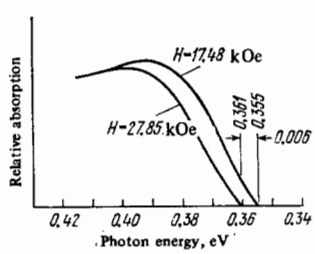

FIG. 11. Dependences of the band intensities of cyclotron resonance in diamond on the energy of photons exciting carriers of effective mass $1.06m_0$ (left-hand curve) and $0.70m_0$ (right-band curve).[19]

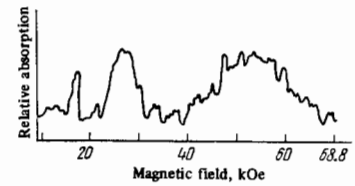

FIG. 12. Cyclotron resonance signal of a natural semiconducting p-type diamond at a frequency of 69.9 GHz and a temperature of 1.55 °K in a field of 68.8 kOe.[19]

The cyclotron resonance data were used in[20] to calculate the density-of-states effective mass. In the case of a spherical band, the carrier density in the band was found to be given by the expression

$$p_t = \frac{1}{2\pi}\exp\left(\frac{E_F - E_V}{kT}\right)\left(\frac{2\pi m_t^* kT}{h^2}\right)^{3/2}, \quad (2)$$

where E_F is the Fermi energy and E_V is the energy corresponding to the bottom of the valence band.

Since there are three valence bands in diamond, we can use Eq. (2) if m^* is replaced with the density-of-states effective mass which allows for the contribution of all three bands. Calculations of this kind were carried out for four values of the coefficient C^2 in Eq. (1).

The calculated values of m^*/m_0 and the corresponding values of C^2 were as follows

C^2:	0	0.06	0.12	0.18
$\frac{m^*}{m_0}$:	3.58	3.66	3.95	4.77.

In this case, m^* denotes the density-of-states effective mass.

The cyclotron resonance experiments were preceded somewhat by an investigation of the temperature dependence of the Hall effect in semiconducting diamonds.[21] An analysis of the dependence of the Hall coefficient on the reciprocal of temperature in the range close to 1000 °K gave the density-of-states effective mass $0.5m_0$. In the subsequent measurements of the Hall effect on samples with fewer defects,[15] it was found that $m^* = 1.1m_0$.

Thus, the experimental values of the density-of-states effective mass found by two different methods disagreed by an amount exceeding a possible experimental error or inaccuracy of the calculations. It was pointed out in[20] that this discrepancy could be eliminated by assuming that the relaxation time in the split-off band was considerably longer than the relaxation times in the two degenerate bands. Since the split-off band was almost spherical, the density-of-states effective mass deduced from the Hall effect should be equal to the cyclotron mass in the split-off band, as found experimentally. The shorter relaxation times of the light and heavy holes should be manifested in the cyclotron resonance experiments as the broadening of the corresponding resonance maxima. This was not observed in[18]. However, we should bear in mind that

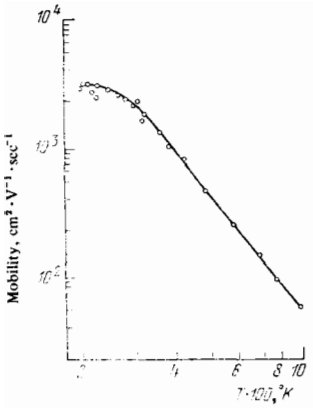

FIG. 13. Temperature dependence of the mobility of holes in a natural semiconducting diamond.[16]

the scattering of carriers at room and higher temperatures should be different from the scattering mechanism at 4 °K. In the latter case, the scattering by ionized impurities should predominate. Therefore, the differences between the relaxation times were manifested particularly in the Hall effect measurements.

No investigations of the conduction band of diamond have yet been made by the cyclotron resonance method.

D. Mobility of electrons and holes in diamond. Photoionization and ionization by charged particles

The mobility of holes in diamond was determined mainly by measuring the Hall effect in natural semiconducting crystals.[21,15] The most reliable measurements of the hole mobility were reported in[15], where it was found that at 300 °K the mobility was $\mu_H = 1550 \pm 150$ cm$^2 \cdot$ V$^{-1} \cdot$ sec^{-1}.

Figure 13 shows the temperature dependence of the hole mobility. Near room temperature, the mobility varies as $T^{-3/2}$, which indicates scattering by acoustic lattice vibrations. At higher temperatures, the dependence is $T^{-2.8}$. It is pointed out in[15] that the dependence $\mu_H \propto T^{-2.8}$ can be explained by the interaction of carriers with optical phonons.

Measurements of the magnetoresistance of semiconducting diamond crystals in strong magnetic fields (up to 170 kG) were used in[22] to determine the hole mobilities in the three bands at room temperature on the assumption that these bands were spherical. The mobilities were found to be 3900, 195, and 1365 cm$^2 \cdot$ V$^{-1} \cdot$ sec^{-1} in the light- and heavy-hole bands and in the split-off band, respectively. The scattering was attributed to the interaction with the acoustic lattice vibrations.

Measurements of the electron mobility in diamond involve special difficulties. Electrons in the conduction band can be created only by excitation with light or with ionizing radiation. The photoconductivity of diamond usually increases with decreasing wavelength. In the visible range, the photoconductivity of diamond is very weak. Figure 14 shows the dependence of the photoconductivity of diamond on the wavelength in the ultraviolet part of the spectrum.[23] In this case, the measurements were carried out on a p-type semiconducting diamond and on insulating crystals. Similar results were obtained in[24] for insulating diamonds. Beginning from the wavelength of 2350 Å, the photoconductivity is associated with transitions to exciton states, whereas, at longer wavelengths, the photoconductivity is of impurity origin.

Current pulses can be created in diamond by nuclear radiations such as α particles or electrons. The energy needed to create an electron–hole pair was determined most accurately in[25] and found to be 16 ± 0.4 eV. As in the case of silicon and several other semiconductors, this value was approximately three times as large as the forbidden band width.

Measurements of the Hall effect in optically excited insulating crystals were reported in[26–28]. The Hall mobility of electrons measured in various samples exhibited considerable scatter. According to[28], the mobility at 300 °K varied from sample to sample in the range from 900 to 2000 cm$^2 \cdot$ V$^{-1} \cdot$ sec^{-1}. The temperature dependence of the mobility in the range 300–450 °K was the same for all the samples and was described by the law $\mu_H \propto T^{-3/2}$.

Clearly, this scatter of the mobility values could not be explained by different mechanisms of carrier scattering in different samples. It was shown in[28] that the scatter of the mobilities should be attributed to an inhomogeneous distribution of the nonequlibrium carrier density along a sample, which was either due to an inhomogeneity in the distribution of the impurity atoms from which electrons were excited to the conduction band or due to variations in the lifetime. It was concluded in[28] that the Hall mobility of electrons in diamond at 300 °K, governed by the scattering of carriers on acoustic lattice vibrations, was 2000 ± 100 cm$^2 \cdot$ V$^{-1} \cdot$ sec^{-1}. Attempts to determine the drift mobility of electrons and holes were made in[29]. Current pulses were created by bombarding a diamond crystal with α particles and the parameters of these pulses were determined as a function of the voltage applied to the sample. However, the mobilities of 3900 cm$^2 \cdot$ V$^{-1} \cdot$ sec^{-1} for electrons and 4800 cm$^2 \cdot$ V$^{-1} \cdot$ sec^{-1} for holes were strongly overestimated and this occurred because the dependence of the mobility on the electric

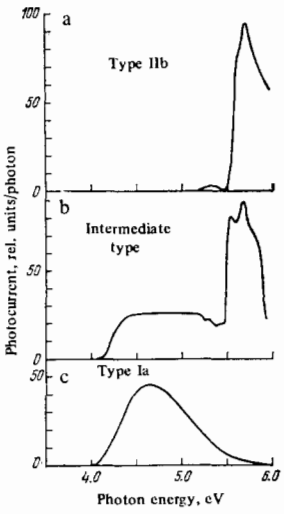

FIG. 14. Photoconductivity spectra of diamond (recorded at 90 °K)[22]: a) natural semiconducting crystal (type IIb); b) insulating crystal with a low nitrogen concentration ($< 10^{19}$ cm^{-3}); c) crystal with high nitrogen concentration (type Ia).

field was ignored in[29].

The dependences of the electron and hole mobilities on the electric field were investigated in[28]. Measurements were made of the Hall effect when carriers were excited optically by photons of energy smaller than the forbidden band width of diamond. At 120 °K, the electron mobility began to decrease in a field of 500 V/cm and depended on the field as $1/\sqrt{E}$. From about 1500 V/cm, the field dependence became stronger and, at about 4×10^3 V/cm, it was found that $\mu_H \propto 1/E$. This corresponded to the drift velocity saturation. At room temperature, the influence of the field on the mobility started at higher fields of 2×10^3 V/cm. The experimental difficulties[28] made it impossible to obtain the dependence $\mu_H \propto 1/e$ at room temperature. A different method was used in[30] to show that the drift velocity saturated at room temperature in a field of 10^4 V/cm and that the maximum drift velocity was 10^7 cm/sec. The electric field in which the mobility began to decrease was in good agreement with the results of calculations based on the existing theories. The drift velocity saturation observed experimentally for diamond was even more difficult to explain than in the case of germanium or silicon.

The energy of optical phonons in diamond is approximately 0.16 eV. In a field of 10^4 V/cm, the number of electrons of this energy is negligible so that the transfer of energy to the lattice in the form of optical phonons (assumed in the theory) is difficult. We cannot even invoke the mechanism of energy accumulation by the electron–electron interaction since the electron density in the conduction band of dimond is also very low.

3. NATURAL p-TYPE SEMICONDUCTING DIAMONDS

Natural semiconducting diamonds always have p-type conduction. Since natural semiconducting diamonds are only encountered in very small quantities, they have no practical applications. However, the majority of the physical investigations described in the preceding section was carried out on these natural semiconducting diamonds. This was also true of the investigations of the properties of acceptor impurity centers in diamond.

A. Ionization energy and excited states of acceptors

The first measurements of the optical and electrical properties of semiconducting diamonds were made

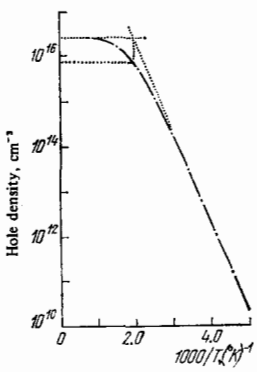

FIG. 15. Temperature dependence of the free-carrier density[15] in a diamond sample ($2.93\times1.52\times1.52$ mm) with $N_a-N_d=(2.6\pm0.3)\times10^{16}$ cm^{-3}, $N_a=(3.2\pm0.3)\times10^{16}$ cm^{-3}, $N_d=(5.6\pm1.2)\times10^{15}$ cm^{-3}.

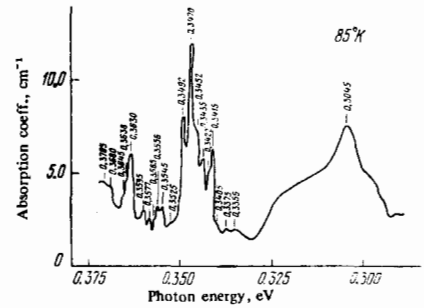

FIG. 16. Optical absorption spectrum of semiconducting diamond at 85 °K.[34]

in[21,31,32] and continued on more carefully selected samples in[15,33,34].

Figure 15 shows the dependence of the free-carrier density on the reciprocal of temperature.[15] The acceptor N_a and donor N_d concentrations were deduced from this dependence by a graphical method (shown dotted). The ionization energy of acceptors was 0.369 + 0.007 eV. This ionization varied from sample to sample between 0.29 and 0.37 eV. The net impurity concentration (N_a-N_d) was usually within the range 10^{15}–10^{17} cm^{-3}. The scatter of the ionization energies could be due to the inhomogeneity of the impurity distribution and, consequently, inaccuracy of the measured Hall coefficient, or it could be due to mechanical stresses in a crystal.

Figure 16 shows the infrared absorption spectrum of diamond.[34] In the range 0.2–0.32 eV, there is a superposition of the absorption due to the lattice vibrations.[35] Clear maxima are due to transitions of holes from the ground to excited states. A continuum begins at about 0.37 eV and this continuum is due to the photoionization of holes. The maxima in Fig. 16 can be combined in pairs and the peaks in each pair are separated by 0.002 eV. Since at 5 °K the high-energy component of a pair increases and the low-energy arc almost disappears,[36] there are grounds for assuming that 0.002 eV is the spin–orbit splitting of the ground state of acceptors. The optical absorption of diamond under uniaxial compression was also investigated in[34].

Strictly speaking, the effective mass approximation cannot be applied to diamond. The Bohr radius of the ground state, estimated from the formula

$$\rho=\frac{\varepsilon\hbar^2}{m^*e^2},$$

where m^* is the effective mass and ε the permittivity, is approximately 4 Å ($m^*/m_0\sim1$). This small value of the Bohr radius of acceptors excludes the possibility of using the above formula. Therefore, there is as yet no complete theory of acceptor states in diamond. However, the effective mass approximation and the theory of groups were used in[34] in a qualitative analysis of the excited states of acceptors in diamonds whose binding energies were considerably lower. They were able to construct a scheme of hole transitions interacting with photons, which agreed with their own experimental results on uniaxial compression and with the temperature dependence.

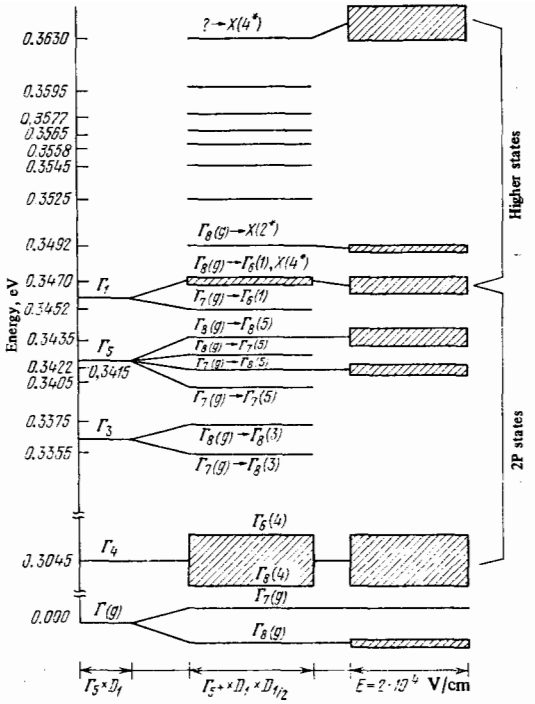

FIG. 17. Energy levels of acceptor states in semiconducting diamond. The first column gives the level position without allowance for the spin–orbit splitting, the second with allowance for the splitting, and the third shows the influence of an applied electric field on the levels.[36]

Confirmation of the transition scheme proposed in[34] was obtained by investigating the Stark effect in acceptors in diamond.[37] It was assumed that the Stark effect in the ground state of an acceptor was less than that found experimentally and, therefore, the shift and splitting of the absorption maxima in an electric field were attributed to the Stark effect in excited states. The data on the splitting (or broadening) and shift of the optical absorption maxima could be used to find the degree of degeneracy of a given state: the line shift alone indicated double degeneracy but the shift and splitting (or broadening) taken together indicated quadruple degeneracy. The transition scheme proposed in[34] is given in Fig. 17 (taken from[37]) together with the data on the Stark effect. All the energies are measured from the ground state of the acceptors. The first excited state is represented by a wide band with its center at 0.3045 eV. This state should have two unresolved levels and one of them should be quadruply degenerate and the other doubly degenerate. In an electric field, this shaded band shifts and broadens, which may be explained by a parallel shift of both levels and broadening of one of them. However, the large width cannot be explained by the superposition of two overlapping bands. We have to adopt the assumption, suggested in[33], relating the large band width 0.304 eV to the reduction in the hole time at the excited levels in question. A hole excited to the 0.304 eV level is transferred almost instantaneously to another level to which transitions from the ground state are forbidden.

The validity of the treatment of the excited states on the basis of the effective mass approximation was also confirmed by the data on the Zeeman effect in acceptor states in diamond.[38] A detailed investigation was made of the splitting of the 0.347 and 0.349 eV levels in a magnetic field.

The continuous absorption, which begins from the photon energy 0.37 eV and is associated with the photoionization of holes, extends far into the visible range, gradually decreasing in intensity. This absorption is responsible for the blue color of semiconducting diamonds. Fairly clear maxima at energies of 0.462, 0.508, 0.625, and 0.670 eV can be seen against the continuous absorption. These maxima can be explained satisfactorily by transitions to excited states at 0.304, 0.347 and 0.363 eV accompanied by the emission of a transverse optical phonon whose energy is about 0.16 eV.

The participation of phonons in electron transitions in semiconducting diamonds is manifested even more clearly in the photoconductivity spectrum.[39] Figure 18 shows the photoconductivity spectrum of a semiconducting diamond. The low-energy edge corresponds to the ionization energy of the acceptors. A complex structure is observed at higher energies. Clear photoconductivity minima (d and e, and d' and e' in Fig. 18) differ from the absorption peaks at 0.304 and 0.347 eV by 0.161 and 2×0.161 eV, i.e., by multiples of the optical phonon energy. The appearance of these minima is related to a reduction in the free-carrier lifetime at the indicated photon energies. If an optically liberated hole acquires from a photon an energy in excess of the excited-state energy and this excess is a multiple of the optical phonon energy, there is an increase in the probability of capture of a hole by this excited acceptor state and of simultaneous emission of a phonon. Holes are captured mainly by the excited states at 0.304 and 0.347 eV.

B. Nature of acceptor centers

Investigations of the optical and electrical properties of a fairly large number of natural semiconducting diamonds have shown that the acceptor responsible for these properties is of the same nature. Until recently, it was assumed that this acceptor was an aluminum atom replacing a carbon atom at a lattice site. Natural diamonds always contain aluminum and this impurity is sometimes present in high concentrations.[40] The great scarcity of semiconducting diamonds has been

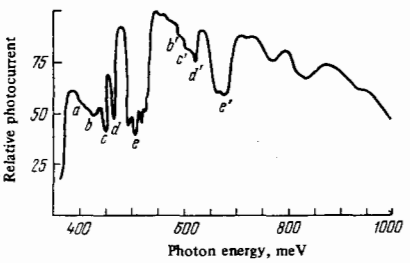

FIG. 18. Photoconductivity spectrum of a semiconducting diamond crystal at 77 °K.[39] The maximum e' is a two-photon replica of the minimum e, etc.[39]

TABLE 3. Aluminum content ($\times 10^{-9}$), g.

Sample	From Hall effect	From activation analysis	
		Experiment I	Experiment II
D 114	20.8±1.0	1.5±0.4	1.1±0.4
D 119	49.4±2.0	1.6±0.4	2.0±0.4
SA 65C	5.2±0.2	1.2±0.4	0.8±0.4
SA 65E	18.1±1.0	1.4±0.4	0.6±0.4
CS 2	55.3±3.0	13.7±0.7	13.3±0.7

attributed to the fact that all diamonds contain also large amounts of nitrogen which may reach 1 at. %. Like group V impurities, nitrogen is a donor (it forms a deep level in diamond) and it compensates acceptors. However, this interpretation was not accepted as final in[41]. Doubts also arose about some properties of synthetic diamonds, which will be discussed later.

The most reliable information on the nature of acceptors in natural semiconducting diamonds was reported in[42]. Measurements were made of the Hall effect in the temperature range 150–1250 °K, of the infrared absorption, and of the aluminum content (by neutron-activation analysis). Table 3 gives the aluminum content found by activation analysis and the concentration of acceptor centers deduced from the Hall effect.

The data in Table 3 are fully convincing: it follows from them that the concentration of aluminum atoms is less than the acceptor concentration (in some crystals by one order of magnitude).

This information is in conflict with earlier hypotheses on the role of aluminum as the dominant acceptor in diamond. It is suggested in[42] that the most probable impurity responsible for the semiconducting properites of diamond is boron. The data obtained for synthetic semiconducting diamonds doped during growth or by the ion implantation method confirmed this suggestion.

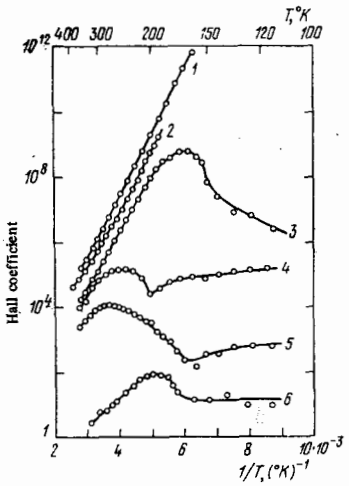

FIG. 19. Dependence of the Hall coefficient (cm^3/C) on the reciprocal temperature.[48] The scales for the different curves are as follows: 1) ×10; 2) ×3; 3) ×1; 4) ×1; 5) $\times 10^{-1}$; 6) $\times 10^{-2}$. 1) natural diamond; 2) aluminum-doped sample; 3)–6) boron-doped samples.

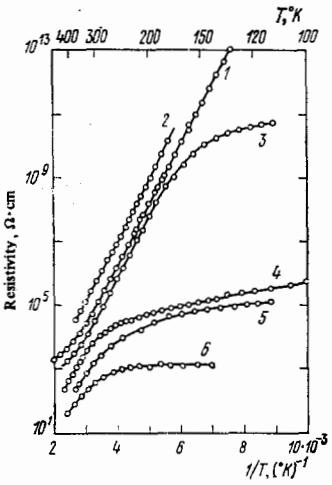

FIG. 20. Dependence of the electrical resistivity on the reciprocal temperature.[48] The designations are the same as in Fig. 19.

C. Thermoelectric power

Measurements of the thermoelectric power of semiconducting diamonds were carried out in the temperature range 200–700 °K.[43] At 300 °K, this power was 3.5 mV/deg. An analysis of the experimental results showed that, below 300 °K, the thermoelectric power was dominated by the component α_p, which was due to the drag of electrons by phonons. At 200 °K, the drag component α_p for diamond was 1.1×10^{-2} V/deg (the corresponding component for silicon was 1.2×10^{-3} V/deg).

4. SYNTHETIC SEMICONDUCTING DIAMONDS

Some years ago, after the successful synthesis of diamonds,[44] Wentorf and Bovenkerk[45] and Huggins and Cannon[46] grew semiconducting diamonds. The dopants were boron, aluminum, and beryllium. When crystals of sufficiently high quality were obtained, fairly detailed investigations of their properites were made. The electrical properties were investigated in[47–51].

Figure 19 shows the dependences of the Hall coefficient on the reciprocal temperature obtained for various samples.[48] Figure 20 gives the dependences of the resistivity of the same samples on the reciprocal temperature.

The results obtained indicated[48] that the ionization energy of acceptors was the same in all samples. Different values of the activation energy of conduction could be due to the concentration dependence of the ionization energy or due to the occurrence of hopping conduction. It should be noted that all the samples doped deliberately with boron contained large amounts of aluminum.

Measurements of the infrared absorption in synthetic semiconducting diamonds were reported in[52,53].

Figure 21 shows part of the absorption spectrum of natural and synthetic diamonds.[52] In this range of photon energies, the absorption is due to transitions of the third and fourth excited states of acceptors. It is clear from Fig. 21 that the absorption spectra are identical except that the spectrum of synthetic diamond

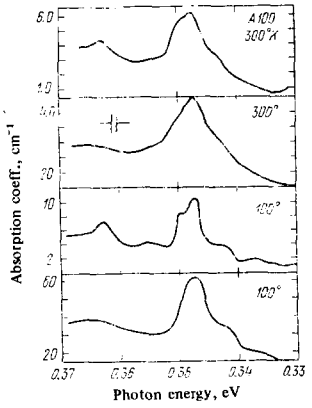

FIG. 21. Absorption spectra of semiconducting diamonds: natural A100 crystal (first and third curves from the top) and synthetic crystal (second and fourth curves from the top).[52]

is broader.

Thus, investigations of synthetic diamonds carried out in the period 1962–1970 indicated that natural and synthetic crystals, the latter doped with aluminum and boron, contained the same acceptor. Since aluminum was present in all these diamonds, it was concluded that the acceptor in diamond was aluminum. Boron was attributed a level separated by a smaller gap from the top of the valence band and, therefore, it should be the first to be compensated by impurities. However, it was not clear why an increase in the aluminum concentration did not result in a considerable reduction in the resistivity, whereas the introduction of boron produced this effect.

In addition to electrical and optical properties of synthetic diamonds, studies were also made of ESR spectra.[54] These spectra had two wide bands which were attributed in[54] to resonant absorption by free and bound holes. Quantitative estimates were not obtained because of the poor quality of the samples.

A considerable change in the status of synthetic diamond occurred in 1971, when it was shown[51,56] that diamond crystals free of inclusions and strong stresses could be grown in the laboratory and that crystals obtained in this way had relatively small amounts of accidental impurities ($< 10^{16}$ cm^{-3} nitrogen). Crystals grown in this way were up to 1 carat in weight. Semiconducting crystals were also grown by simultaneous doping with aluminum and boron. The authors themselves pointed out that these diamonds were more expensive than natural stones but they had exceptional properties suitable for investigations and applications in electronics.

Figure 22 shows the temperature dependences of the thermal conductivity of synthetic and natural diamonds of various classes.[56] We can see that the thermal conductivity of synthetic diamonds exceeds the thermal conductivity of the best natural samples, which shows that there are fewer defects in the former. The nature of the acceptors was also solved in the investigations mentioned above. Figure 23 shows the absorption spectra of a diamond sample not specially doped but containing nitrogen, a sample doped with aluminum, and a sample doped with aluminum and boron. Only in the latter case does the spectrum include absorption

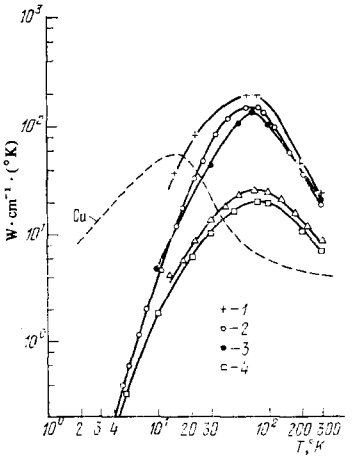

FIG. 22. Temperature dependences of the thermal conductivity of synthetic and natural diamonds.[58] Synthetic diamonds: 1) nitrogen-doped, 10^{16} atoms/cm^3; 2) nitrogen-doped, 10^{-2} at.%. Natural diamonds[1]: 3) type IIa (low nitrogen concentration); 4) type Ia (3.5×20^{20} atoms/cm^3); △) type Ia and IIa; the classification of diamonds is the same as in[1].

typical of semiconducting diamond. The role of aluminum clearly reduces to the binding of nitrogen during growth so that the boron acceptor does not become compensated. It is shown in[57,58] that titanium plays the same role as aluminum. In samples free of macroinclusions, the aluminum concentration is very slight: its solubility in diamond is clearly low. Therefore, the results reported in[56] do not exclude aluminum as one of the possible acceptors in diamond.

The infrared spectra of synthetic diamonds doped with arsenic were investigated.[57] The spectra had new strong absorption bands at 0.351 and 0.507 eV. Unfortunately, electrical measurements were not carried out on these crystals.

Synthetic semiconducting diamonds also include boron-doped diamond films which grew on the surfaces of grain powders from natural diamond at a pressure of 0.1–1 Torr and a temperature of 1050 °C, i.e., under conditions such that diamond was thermodynamically metastable.[59] In this case, diamond grew epitaxially from the gaseous phase containing a mixture of diborane and methane. Initially, attempts to grow such films on single crystals of natural diamond were not

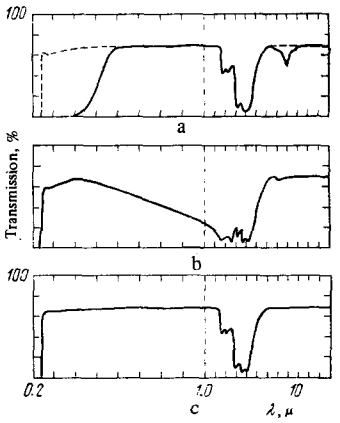

FIG. 23. Absorption spectra of synthetic diamonds[56]: a) high nitrogen concentration; b) doped with aluminum and boron; c) doped with aluminum alone. The vertical dashed line represents the change in scale along the wavelength axis.

successful.[59] However, it was shown later[60] that epitaxial growth from the gaseous phase could be used to obtain single-crystal films of an area amounting to several square millimeters.[60] Although the films investigated in[60] were not specially doped, it should be possible to prepare semiconducting films by this method in the near future.

5. NITROGEN CENTERS IN DIAMOND

The second impurity, after boron, which can easily be incorporated in the diamond lattice in large quantities (up to 1 at.%) is nitrogen.[61] Clearly, like boron, nitrogen replaced carbon atoms in the lattice. Since nitrogen belongs to group V, it should be a donor. However, all diamonds containing larger amounts of nitrogen are good insulators.

Isolated nitrogen atoms replacing carbon appeared in the ESR spectrum in the form of characteristic absorption bands.[62] An analysis of the ESR spectra showed that the donor electron was strongly localized, i.e., the energy level was located at a considerable distance from the bottom of the conduction band. Therefore, the density of free electrons in the band at moderate temperatures was practically equal to zero.

The concentration of isolated nitrogen atoms in natural diamond was found to represent only a small fraction of the total concentration but the ratio of the two concentrations was usually constant and equal to 2×10^{-5} for various crystals.[63] Thus, most of the nitrogen present in natural diamond was found to form complex aggregates. The centers composed of two paired nitrogen atoms[67] and large complexes composed of two layers of nitrogen atoms were among those identified most reliably. The latter complexes were platelets oriented in the (100) plane.[68] The two types of center were nonparamagnetic. It was interesting to note that the converse was true of synthetic diamonds in which the nitrogen was present mainly in the form of single isolated atoms.[64] Clearly, the crystal growth conditions in nature and laboratory were very different.

The presence of nitrogen was responsible for a wide ultraviolet absorption band, which started at a photon energy of about 4 eV and merged with the fundamental absorption of diamond.[1] Photoconductivity was observed in the same part of the spectrum and the photocarriers were electrons.[24] This indicated that the ionization energy of the nitrogen donors was about 4 eV. This energy probably depended on the form in which the nitrogen was present. Therefore, the absorption and photoconductivity spectra were wide bands.

The nitrogen impurity in diamond gave rise to local lattice vibrations which were optically active and responsible for infrared absorption. The nature of the absorption spectrum of these local vibrations depended on the predominance of a given form of nitrogen and could differ from crystal to crystal.

A calculation of the ionization energy of nitrogen donors in diamond was reported in[65]. Use was made of the method of combinations of atomic and molecular orbitals. The same method was employed in a preliminary calculation of the energy band structure of pure diamond. Since a limited number of carbon atoms was used in these calculations, the valence and conduction bands were found to consist of discrete although closely spaced levels. The energy gap between the bands predicted by these calculations was close to the experimental value. The ionization energy of the nitrogen donors was 4 eV.

There have been many investigations of nitrogen impurities in diamond (these are reviewed in[69]).

Modern analytic methods have revealed not only boron and nitrogen but also many other elements in amounts of 10^{17}–10^{16} cm^{-3} in diamonds. However, there is no evidence of the influence of these elements on the physical and optical properties of diamond. It is not clear, also, how these impurities are captured by the diamond lattice. It is possible that, like aluminum, these impurities are present mainly as macroinclusions and as a result the diamond crystals are much purer than hitherto assumed.

The greatest interest lies in the behavior of group V impurities in diamond, i.e., phosphorus, arsenic, etc. Like nitrogen, these impurities should be donors. However, *n*-type semiconducting diamond crystals have not yet been encountered in nature or produced in the laboratory (except by implantation).

6. SEMICONDUCTING DIAMONDS PREPARED BY ION IMPLANTATION METHOD

Attempts to diffuse impurities into diamond crystals, so as to impart semiconducting properties, have not been successful. Diffusion in diamond begins only at very high temperatures (exceeding 1500°C), when diamond is no longer stable under normal pressure. It is reported in[70] that semiconducting films were prepared under pressure at high temperatures by the diffusion of boron into natural diamond. However, it was not clear whether this was the true diffusion of boron or epitaxial growth of a semiconductor film on the surface of the original crystal.

In recent years, it has become usual to introduce impurities by implantation of accelerated ions. The advantages of the implantation method are well known. The main and, unfortunately, unavoidable shortcoming is the large number of displacements of atoms from their sites in the original crystal. Therefore, success in the application of this method to diamond depended on the possibility of restoring the crystal structure by subsequent annealing.

The first short report, by American workers, of ion implantation in diamonds appeared in 1965[71] followed by the Soviet report in 1966.[72] The subsequent investigations of the electrical conductivity of implantation-doped diamond layers subjected to high-temperature annealing,[73] channeling of high-energy protons in diamond,[74] and paramagnetic resonance[75] demonstrated that the lattice damage caused by implantation could be largely healed by annealing at 1400°C.

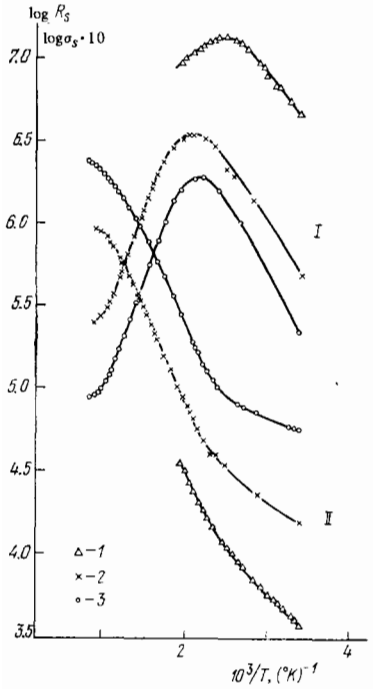

FIG. 24. Dependence of the Hall coefficient R_s(I) and electrical conductivity (II) of a diamond layer containing implanted boron ions (ion energy 55 keV, dose 1.7×10^{15} cm^{-2}), and annealed at various temperatures (°C): 1) 1000; 2) 1150; 3) 1350.

The most detailed investigations were made of p-type semiconducting layers prepared by the implantation of boron acceptors.[76]

During the early stages of annealing, the implanted boron atoms occupy lattice sites and do not diffuse even at high temperatures. Figure 24 shows the dependences $\log\sigma_s = f(1/T)$ and $\log R_s = f(1/T)$ taken from[76]. Here, σ_s is the surface conductance, i. e., the conductance of 1 cm^2 of the layer, R_s is the effective Hall coefficient given by $R_s = 1/ep_s$, and p_s is the number of carriers per 1 cm^2 of the layer. The measurements were carried out during various stages of annealing. According to Fig. 24, the annealing of defects occurred up to 1350–1400 °C since the free carrier density and the conductance increased between the annealing stages. The Hall coefficient R_s exhibited a maximum and the dependence $\log\sigma_s = f(1/T)$ had a change in slope at the temperature of this maximum. This demonstrated that, below 600 °K, the conduction process in the sample was of the interimpurity (hopping) type. This was in agreement with the high acceptor concentration in the layer, which amounted to about 10^{19} atoms/cm^3. The ionization energy of acceptors governed the slope of the high-temperature part of the dependence $\log R_s = f(1/T)$. The values of the ionization energy, mobility, and surface concentration of uncompensated acceptors in several samples are listed in Table 4. It follows from this table that the mobilities may be fairly high. The ionization energy (0.3 eV) is close to the ionization energy of acceptors in natural diamonds.[79]

The implantation of lithium ions in diamond is of particular interest because the first n-type semiconducting diamond crystals were produced in this way.

An investigation of the distribution of implanted lithium in diamond established that the position of the concentration maximum was in agreement with the theory.[77] However, some of the ions were found at depths much greater than those predicted theoretically. Near the concentration maximum, the lithium was in a strongly disordered layer, whereas, in the "tail" of the distribution curve of lithium, the concentration of defects was relatively low. This was probably why annealing of implanted layers had a different effect in the region of the maximum concentration of lithium and in the tail region.[78] When the annealing temperature was increased, the electrical conductivity of diamond in the layer corresponding to the lithium concentration maximum decreased, whereas, in the region of the tail, it increased. After annealing at 1400 °C, the overall conductivity of the lithium-doped diamond layer was several orders of magnitude higher than the conductivity of the same layer immediately after implantation. The conducting layer was located at a depth 2–3 times higher than the depth of the lithium concentration maximum and was separated from the surface by an insulating layer. Figure 25 shows how the conductivity varied as a result of layer-by-layer etching of an im-

TABLE 4.

Sample No.	Radiation dose, ions/cm^2	Resistivity of layer ($\Omega\cdot$cm) at $T=300$ °K	$N_{as}-N_{ds}$ (extrapolated)	Mobility, cm$^2\cdot$V$^{-1}\cdot$sec^{-1}		Comments
				$T=300$ °K	$T=600$ °K	
			Boron			
13K	$1.7\cdot10^{15}$	6	$1.5\cdot10^{14}$	1	40	Hopping conduction in sample 13 K at 300 °K
80	10^{15}	6	$5\cdot10^{13}$	30	100	
78	$6\cdot10^{14}$	13.5	10^{13}	500	180	
82	$6\cdot10^{14}$	13.5	$4\cdot10^{13}$	700	180	
72	$3\cdot10^{14}$	30	$2\cdot10^{13}$	400	110	
			Lithium			
62M	$1.2\cdot10^{15}$	0.6	–	–	–	Results of ac measurements
67M	$6\cdot10^{15}$	0.8	–	–	–	
65	$1.2\cdot10^{15}$	1.2	–	–	–	
65	$3\cdot10^{16}$	1	–	–	–	
132	$1.2\cdot10^{15}$	10^4	–	–	–	
132	$6\cdot10^{15}$	10^3	–	–	–	

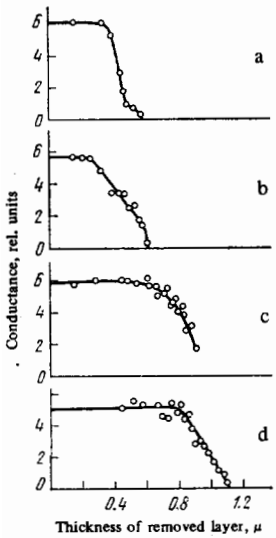

FIG. 25. Dependences of the surface conductance of layers on four samples implantation-doped with lithium during successive etching away. The dose was 3 $\times 10^{16}$ cm^{-2} and the energy (keV) was 40 for samples a–c and 80 for sample d. Sample b was annealed for 30 h at 1400 °C.

plantation-doped sample.[78] The anomalous distribution of the lithium atoms and conductivity has not yet been fully accounted for.

It is very difficult to form ohmic contacts needed in investigations of the Hall effect at $p-n$ junctions in diamond; a fully satisfactory technique has yet to be developed. This is clearly due to the fact that the energy barrier at the boundary between n-type diamond and a metal (aluminum or gold) is very high, being much higher than the corresponding barrier on silicon.

Table 4 gives the values of the resistivity of doped layers formed by implantation of various lithium ion doses. Clearly, the resistivity is poorly correlated with the dose. Some (relatively few) samples have a high resistivity and this may be due to the presence of accidental compensating impurities.

The dependence $\log\sigma_s = f(1/T)$ is a straight line; the activation energy of conduction is 0.17 eV.

Semiconducting n-type layers were formed in diamond by implantation of carbon and group V ions.[73,81] However, annealing above 800 °C destroyed this type of conduction. Annealing at 800 °C or lower resulted in the retention of some of the radiation defects. Layers obtained in this way were strongly compensated low-mobility semiconductors. In spite of that, the implantation of boron and phosphorus ions into a diamond plate produced the first $p-n$ junction in diamond.[80] A structure with a $p-n$ junction is shown in Fig. 26. The $p-n$ junction plane was perpendicular to the planes

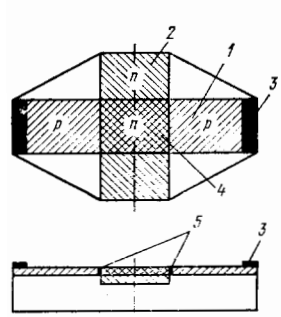

FIG. 26. Sample with a $p-n$ junction: 1) p-type region with implanted boron; 2) n-type region with implanted phosphorus; 3) ohmic contact; 4) n-type region with boron overcompensated by phosphorus; 5) $p-n$ junctions.

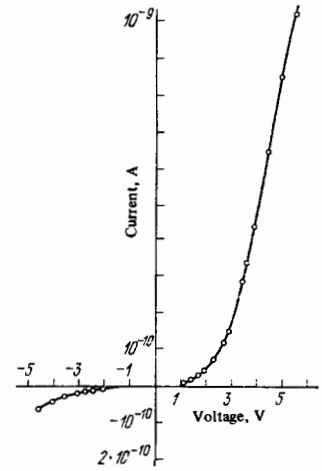

FIG. 27. Current-voltage characteristic of a $p-n$ junction.

of the doped p- and n-type layers; the area was approximately 2×10^{-6} cm^{-2}.

Figure 27 gives the current-voltage characteristic and Fig. 28 the photo-emf spectrum obtained as a result of illumination of this $p-n$ junction with ultraviolet light. The photosensitivity was found to lie in the range of wavelengths corresponding to the fundamental absorption edge of diamond.

It is difficult to say why implantation of group V elements fails to produce electrically active donors in diamond. It is possible that the replacement of carbon at a lattice site results, by analogy with nitrogen, in deep donor levels. Moreover, these elements may not behave as substitutional impurities. For example, it was reported in[74] that, after annealing at 900 °C, the implanted phosphorus atoms were not located at the lattice sites. Such studies have not yet been carried out after annealing at higher temperatures.

7. POTENTIAL PRACTICAL APPLICATIONS OF SEMICONDUCTING DIAMONDS

The preparation of high-quality synthetic semiconducting diamond crystals, the success attained in ion implantation doping, and the possibility of epitaxial growth of diamond on diamond provide sufficient evidence to expect the eventual use of this unique material in semiconductor electronics. Devices have already

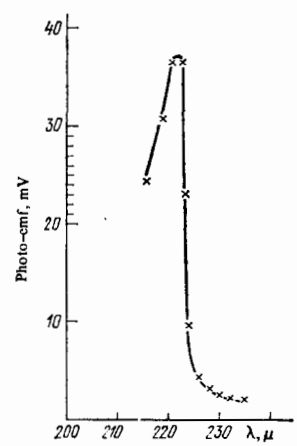

FIG. 28. Dependence of the photo-emf of a $p-n$ junction on the exciting light wavelength.

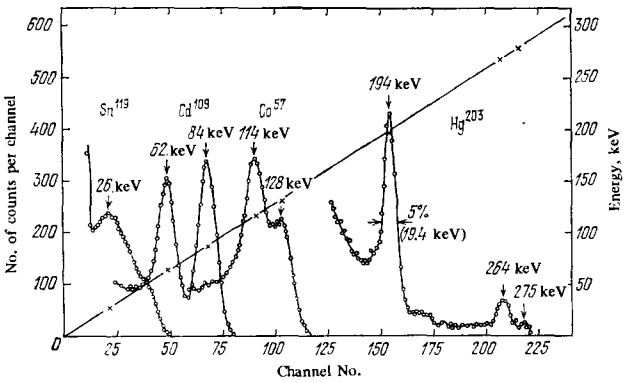

FIG. 29. Energy spectrum of conversion electrons emitted from Sn^{119}, Cd^{109}, Co^{57}, and Hg^{203} nuclides.

been developed on the basis of diamond and these include a nuclear radiation detector[125] and a thermistor.[82]

The active zone of a diamond detector is a high-quality homogeneous insulating natural diamond. The main feature of this new type of detector is the use of contacts which inject carriers into the bulk of the crystal, which avoids polarization in the bulk and ensures operational stability of the detector. Diamond detectors can be used at high temperatures (up to 300°C) and in aggressive chemical media. They have a good radiation stability, which is two orders of magnitude higher than that of silicon detectors (in respect of neutrons); moreover, diamond detectors have the advantage of a low noise level. This makes them suitable for the detection of low-energy nuclear radiations. Figure 29 shows the conversion-electron spectra of various nuclides recorded at room temperature.

The strong temperature dependence of the electrical conductivity, low specific heat, and high thermal conductivity of diamond make it an ideal thermistor, which is sensitive and has a fast response.

The high conductivity of diamond makes it possible to use this material as a heat sink for semiconductor devices (for example, avalanche-transit silicon diodes or semiconductor lasers).[83] The use of such heat sinks makes it possible to increase the power dissipation in semiconductor devices severalfold.

The capacitance-voltage characteristics of Schottky barriers on synthetic p-type diamonds were investigated in[84]. A model was proposed in that paper for the calculation of these characteristics, allowing for the time needed to liberate carriers from an acceptor level to a band and for the series resistance of the semiconductor, which could not be ignored in the case of diamond. The height of the gold–diamond potential barrier was within the range 1.25–1.45 eV, in agreement with the earlier results.[85] This study could provide a foundation for the development of new high-frequency devices.

Natural diamonds luminesce in the ultraviolet and visible parts of the spectrum. The luminescence yield is fairly high: according to[86], the yield of electron-beam-excited diamonds is 0.01–0.03 photons per electron–hole pair. Therefore, $p-i-n$ structures based on diamond are efficient radiation sources.

Only the first steps have been taken in applying semiconducting diamonds in practice. It is at present difficult to predict all potential applications of semiconducting diamonds. They will become clear as the technology for the preparation of the pure material develops; in our opinion, the epitaxial method may become particularly important.

[1]R. Berman (ed.), Physical Properties of Diamonds, Clarendon Press, Oxford, 1965.
[2]F. Herman, R. L. Kortum, C. D. Kuglin, and R. A. Short, Proc. Eighth Intern. Conf. on Physics of Semiconductors, Kyoto, 1966, in: J. Phys. Soc. Jpn. 21, Suppl., 7 (1966).
[3]W. Saslow, T. K. Bergstresser, and M. L. Cohen, Phys. Rev. Lett. 16, 354 (1966).
[4]H. Jones, The Theory of Brillouin Zones and Electronic States in Crystals, North-Holland, Amsterdam, 1960.
[5]T. P. McLean, Prog. Semicond. 5, 53 (1956).
[6]C. D. Clark, P. J. Dean, and P. V. Harris, Proc. R. Soc. Ser. A 277, 313 (1964).
[7]R. J. Elliott, Phys. Rev. 108, 1384 (1957).
[8]J. L. Warren, R. G. Wenzel, and J. L. Yarnell, in: Inelastic Scattering of Neutrons (Proc. Third Intern. Symposium, Bombay, 1964), Vol. 1, International Atomic Energy Agency, Vienna, 1965, p. 361.
[9]G. Peckham, Solid State Commun. 5, 311 (1967).
[10]H. R. Philipp and E. A. Taft, Phys. Rev. 127, 159 (1962).
[11]W. C. Walker and J. Osantowski, Phys. Rev. 134, A153 (1964).
[12]H. R. Philipp and E. A. Taft, Phys. Rev. 136, A1445 (1964).
[13]R. A. Roberts and W. C. Walker, Phys. Rev. 161, 730 (1967).
[14]P. J. Dean and I. H. Jones, Phys. Rev. 133, A1698 (1964).
[15]P. J. Dean, E. C. Lightowlers, and D. R. Wight, Phys. Rev. 140, A352 (1965).
[16]V. S. Vavilov, G. P. Golubev, E. A. Konorova, É. L. Nolle, and V. F. Sergienko, Fiz. Tverd. Tela (Leningrad) 8, 1522 (1966). [Sov. Phys.-Solid State 8, 1210 (1966)].
[17]G. Dresselhaus, A. F. Kip, and C. Kittel, Phys. Rev. 98, 368 (1955).
[18]C. J. Rauch, Phys. Rev. Lett. 7, 83 (1961).
[19]C. J. Rauch, Proc. Sixth Intern. Conf. on Physics of Semiconductors, Exeter, England, 1962, publ. by The Institute of Physics, London (1962), p. 276.
[20]P. E. Clegg and E. W. J. Mitchell, Proc. Phys. Soc. London 84, 31 (1964).
[21]P. T. Wedepohl, Proc. Phys. Soc. London Sec. B 70, 177 (1957).
[22]K. J. Russell and W. J. Leivo, Phys. Rev. B 6, 4588 (1972).
[23]P. Denham, E. C. Lightowlers, and P. J. Dean, Phys. Rev. 161, 762 (1967).
[24]E. A. Konorova, L. A. Sorokina, and S. A. Shevchenko, Fiz. Tverd. Tela (Leningrad) 7, 1092 (1965) [Sov. Phys.-Solids State 7, 876 (1965)].
[25]E. A. Konorova and S. F. Kozlov, Fiz. Tekh. Poluprovodn. 4, 1865 (1970) [Sov. Phys.-Semicond. 4, 1600 (1971)].
[26]C. C. Klick and R. J. Maurer, Phys. Rev. 81, 124 (1951).
[27]A. G. Redfield, Phys. Rev. 94, 526 (1954).
[28]E. A. Konorova and S. A. Shevchenko, Fiz. Tekh. Poluprovodn. 1, 364 (1967) [Sov. Phys.-Semicond. 1, 299 (1967)].
[29]E. A. Pearlstein and R. B. Sutton, Phys. Rev. 79, 907 (1950).
[30]E. A. Konorova, S. F. Kozlov, and V. S. Vavilov, Fiz. Tverd. Tela (Leningrad) 8, 3 (1966) [Sov. Phys.-Solid State 8, 1 (1966)].
[31]J. F. H. Custers, Physica (Utrecht) 18, 489 (1952).

[32]I. G. Austin and R. Wolfe, Proc. Phys. Soc. London Sec. B 69, 329 (1956).
[33]S. D. Smith and W. Taylor, Proc. Phys. Soc. London Sec. B 79, 1142 (1962).
[34]P. A. Crowther, P. J. Dean, and W. F. Sherman, Phys. Rev. 154, 772 (1967).
[35]J. R. Hardy and S. D. Smith, Philos. Mag. 6, 1163 (1961).
[36]J. J. Charette, Physica (Utrecht) 27, 1061 (1961).
[37]E. Anastassakis, Phys. Rev. 186, 760 (1969).
[38]D. M. S. Bagguley, S. D. Smith, C. J. Summers, and G. Vella-Coleiro, Proc. Eighth Intern. Conf. on Physics of Semiconductors, Kyoto, 1966, in: J. Phys. Soc. Jpn. 21, Suppl., 244 (1966).
[39]A. T. Collins, E. C. Lightowlers, and P. J. Dean, Phys. Rev. 183, 725 (1969).
[40]E. N. Bunting and A. Van Valkonbury, Am. Mineral. 43, 102 (1958).
[41]P. T. Wedepohl, J. Phys. C 1, 1773 (1968).
[42]A. T. Collins and A. W. S. Williams, J. Phys. C 4, 1789 (1971).
[43]H. J. Goldsmid, C. C. Jenns, and D. A. Wright, Proc. Phys. Soc. London 73, 393 (1959).
[44]F. P. Bundy, H. T. Hall, H. M. Strong, and R. H. Wentorf, Nature (London) 176, 51 (1955).
[45]R. H. Wentorf Jr and H. P. Bovenkerk, J. Chem. Phys. 36, 1987 (1962).
[46]C. M. Huggins and P. Cannon, Nature (London) 194, 829 (1962).
[47]E. C. Lightowlers and A. T. Collins, Phys. Rev. 151, 685 (1966).
[48]A. W. S. Williams, E. C. Lightowlers, and A. T. Collins, J. Phys. C 3, 1727 (1970).
[49]G. N. Bezrukov, V. P. Butuzov, N. N. Gerasimenko, L. V. Lezheĭko, Yu. A. Litvin, and L. S. Smirnov, Fiz. Tekh. Poluprovodn. 4, 693 (1970) [Sov. Phys.-Semicond. 4, 587 (1970)].
[50]L. F. Vereshchagin, O. G. Revin, V. N. Slesarev, I. N. Seĭfi-Khusaĭnov, and A. S. Chmykhov, Dokl. Akad. Nauk SSSR 192, 1015 (1970) [Sov. Phys.-Dokl. 15, 566 (1970)].
[51]Y. F. Tsay, K. P. Ananthanarayanan, P. J. Gielisse, and S. S. Mitra, J. Appl. Phys. 43, 3677 (1972).
[52]A. T. Collins, P. J. Dean, E. C. Lightowlers, and W. F. Sherman, Phys. Rev. 140, A1272 (1965).
[53]Yu. A. Klyuev, V. I. Nepsha, and G. N. Bezrukov, in: Almazy (Diamonds), No. 9, NIIMASh-VNIIALMAZ, M., 1972, p. 1.
[54]J. C. Burgoin, P. R. Brosious, Y. M. Kim, J. W. Corbett, and R. M. Chrenko, Philos. Mag. 26, 1167 (1972).
[55]R. H. Wentorf, J. Phys. Chem. 75, 1833 (1971).
[56]H. M. Strong and R. M. Chrenko, J. Phys. Chem. 75, 1838 (1971).
[57]Yu. A. Klyuev, V. I. Nepsha, and G. N. Bezrukov, Fiz. Tekh. Poluprovodn. 8, 1619 (1974) [Sov. Phys.-Semicond. 8, 1053 (1975)].
[58]L. V. Lezheĭko, Thesis for Candidate's Degree, Institute of Semiconductor Physics, Siberian Branch, Academy of Sciences of the USSR, Novosibirsk, 1972.
[59]D. J. Poferl, N. C. Gardner, and J. C. Angus, J. Appl. Phys. 44, 1428 (1973).
[60]B. V. Deryagin, B. V. Spitsyn, A. E. Aleksenko, A. E. Gorodetskiĭ, A. P. Zakharov, and R. I. Nazarova, Dokl. Akad. Nauk SSSR 213, 1059 (1973) [Sov. Phys.-Dokl. 18, 822 (1974)].
[61]W. Kaiser and W. L. Bond, Phys. Rev. 115, 857 (1959).
[62]W. V. Smith, P. P. Sorokin, I. L. Gelles, and G. J. Lasher, Phys. Rev. 115, 1546 (1959).
[63]E. V. Sobolev, N. D. Samsonenko, and S. V. Lenskaya, Izv. Sib. Otd. Akad. Nauk SSSR Ser. Khim. 3, 156 (1964).
[64]E. V. Sobolev, Yu. A. Litvin, N. D. Samsonenko, V. E. Il'in, S. V. Lenskaya, and V. P. Butuzov, Fiz. Tverd. Tela (Leningrad) 10, 2266 (1968) [Sov. Phys.-Solid State 10, 1789 (1969)].
[65]R. P. Messmer and G. D. Watkins, Phys. Rev. B 7, 2568 (1973).
[66]P. J. Dean, Phys. Rev. 139, A588 (1965).
[67]E. V. Sobolev, V. I. Lisoĭvan, and S. V. Lenskaya, Dokl. Akad. Nauk SSSR 175, 582 (1967) [Sov. Phys.-Dokl. 12, 665 (1968)].
[68]T. E. Evans and C. Phaal, Proc. R. Soc. Ser. A 270, 538 (1962).
[69]G. Davies, in: Diamond Research, London, 1972, p. 21.
[70]W. B. Wilson, Phys. Rev. 127, 1549 (1962).
[71]R. H. Wentorf Jr and K. A. Darrow, Phys. Rev. 137, A1614 (1965).
[72]V. S. Vavilov, M. I. Guseva, E. A. Konorova, V. V. Krasnopevtsev, V. F. Sergienko, and V. V. Titov, Fiz. Tverd. Tela (Leningrad) 8, 1964 (1966) [Sov. Phys.-Solid State 8, 1560 (1966)].
[73]V. S. Vavilov, M. I. Guseva, E. A. Konorova, and V. F. Sergienko, Fiz. Tekh. Poluprovodn. 4, 10 (1970) [Sov. Phys.-Semicond. 4, 6 (1970)].
[74]L. A. Davidson, J. F. Gibbons, R. C. Der, T. M. Kavanagh, and J. M. Khan, Appl. Phys. Lett. 14, 295 (1969).
[75]P. R. Brosious, J. W. Corbett, and J. C. Bourgoin, Phys. Status Solidi 21, 677 (1974).
[76]V. S. Vavilov, M. I. Guseva, E. A. Konorova, and V. F. Sergienko, Fiz. Tekh. Poluprovodn. 4, 17 (1970) [Sov. Phys.-Semicond. 4, 12 (1970)].
[77]B. V. Zatolonin, L. N. Katsaurov, V. V. Krasnopevtsev, Yu. V. Milyutin, and K. Kh. Nusupov, in: Fizihheskie osnovy ionno-luchevogo legirovaniya. Materially nauchnoĭ konferentsii, Gorkiĭ, 1971 (Physical Basis of Ion Implantation Doping-Proc. Scientific Conf., Gorkiĭ, 1971), p. 47.
[78]V. S. Vavilov, M. A. Gukasyan, M. I. Guseva, and E. A. Konorova, Fiz. Tekh. Poluprovodn. 6, 585 (1972) [Sov. Phys Phys.-Semicond. 6, 741 (1972)].
[79]V. S. Vavilov, M. A. Gukasyan, M. I. Guseva, T. A. Karatygina, and E. A. Konorova, Fiz. Tekh. Poluprovodn. 8, 737 (1974) [Sov. Phys.-Semicond. 8, 471 (1974)].
[80]V. S. Vavilov, M. A. Gukasyan, M. I. Guseva, E. A. Konorova, and V. F. Sergienko, Dokl. Akad. Nauk SSSR 200, 821 (1971) [Sov. Phys.-Dokl. 10, 856 (1972)].
[81]V. S. Vavilov, M. A. Gukasyan, E. A. Konorova, and Yu. V. Milyutin, Fiz. Tekh. Poluprovodn. 6, 2384 (1972) [Sov. Phys.-Semicond. 6, 1998 (1973)].
[82]"Blue diamonds make rugged thermistors," Electronics 33, No. 35, 78 (August 26, 1960).
[83]R. Berman, Electron. Eng. 42, No. 510, 43 (1970).
[84]G. H. Glover, Solid-State Electron. 16, 973 (1973).
[85]C. A. Mead and W. G. Spitzer, Phys. Rev. 134, A713 (1964).
[86]P. J. Dean and J. C. Male, J. Phys. Chem. Solids 25, 311 (1964).

Translated by A. Tybulewicz